Naugher LA, Baker NJ, Atkinson G.

Large air gap squirrel cage induction generator for a tidal turbine.

In: 8th IET International Conference on Power Electronics, Machines and Drives (PEMD 2016).

19-21 April 2016, Glasgow, UK: Institute of Engineering and Technology (IET).

DOI link to article:

http://dx.doi.org/10.1049/cp.2016.0333

Date deposited:

27/07/2016

Large air gap squirrel cage induction generator for a tidal turbine

L. A. Naugher*, N. J. Baker*, G. Atkinson*

** Electrical Power Research Group, School of Electrical and Electronic Engineering, Newcastle University*

Keywords: Large air gap, induction generator, Tidal turbine, machine design.

Abstract

An induction generator has been designed for use in an open centred tidal turbine. Mechanical constraints in the turbine design enforces a large magnetic gap in the generator, which inherently limits the power factor. The large diameter of the machine means it is likely to be constructed out of a number of segments, which can each be modelled independently and approximated to either linear segments or individual rotary machines with the same pole to air gap ratio. An analytical tool to design an induction machine for this unique set of requirements is presented and compared to results from commercial software. Detailed design options are investigated using finite element analysis before a final design is presented.

1. Introduction

A tidal turbine is a method of harvesting renewable energy from the ocean tides, if successful this is a new viable energy source alongside established sources such as wind and solar. Tidal stream devices, unlike tidal barrages and dams, have no expensive architecture required to house the turbine. Instead the turbine is situated on the sea bed and extracts energy from the tidal currents. However placing the turbine below the surface increases the difficulty of the turbine and generator maintenance, therefore increasing the operational cost. By designing the generator to be as robust as possible the operational periods between maintenance can be increased. This would reduce the turbine cost in the long term by reducing the number of maintenance cycles over the life of the turbine.

A number of competing tidal turbines exist, and this work focuses on the OpenHydro turbine. This is an open centred turbine with rim mounted permanent magnet synchronous generator (PMSG) with a shaft-less rotor, Figure 1. The rotor is neutrally buoyant and free to rotate in a large flooded gap. It is a direct drive turbine and the absence of a gearbox means there is one less potential failure point in the turbine. The present generator design is a surface mounted permanent magnet machine [1], heavily reliant on rare earth materials to generate the air-gap field. The purpose of this project is to identify possible alternative generator topologies to reduce reliance on this material. One such alternative is the induction machine, which is the focus of this paper.

The size of the turbine and nature of the environment place a number of design constraints on the generator: the size of the magnetic gap, the ability to compete with the performance of the existing generator, capability of variable speed operation and compatibility with the existing mechanical structure of the turbine.

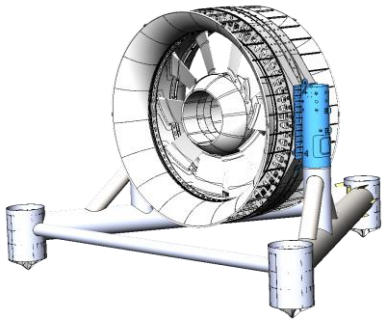

Figure 1: OpenHydro 16m turbine with gravity base [1]

Since its conception in 1888 the squirrel cage induction generator (SCIG) has been used extensively in industry. This was due to its simple construction and the capability to operate in extreme conditions. This generator is capable of variable speed with established control methods and when the machine is disabled no emf is produced by the rotor – good for fault tolerance. However the size of the flooded gap between the rotor and stator in the OpenHydro turbine, which must be large due to mechanical constraints, is a concern in this application. The air-gap increases the leakage inductance thereby decreasing the power factor of the generator. To compensate, an over rated convertor is required. Overall, for the induction machine design to be competitive with the existing PMSG, it needs to have a lower manufacture cost to offset the increased convertor cost as well as competing on physical size and efficiency.

The SCIG has a lower material cost and simpler assembly than the PMSG, due to the absence of rare earth magnets. At rest, the attractive force between the rotor and stator is small and therefore the resistance to rotation is less. The turbine will hence rotate in a lower flow rate. As tidal flow is stationery twice per 12 hour cycle, this increase in operation time could have a significant impact on generation yield over the device lifetime. However, a large airgap results in a SCIG with a worse power factor (PF) and lower efficiency (ŋ) than the PMSG.

2. Design Constraints

The OpenHydro machine studied has a diameter of 14m and a flooded gap of 12mm. Typically an induction machine has an air gap length (l_g) in the range of 0.5 - 4mm. Large induction

machines commonly have efficiencies greater than 90% however a large gap length is known to reduce the efficiency. The large magnetic air gap and physical size of this machine makes using conventional design tools such as Motor Solve inappropriate. Direct drive generators have a large number of poles due to the low angular velocity (<30rpm), the existing PMSG has almost 300 poles.

To make the design physically more manageable, during manufacture the stator of the present design has been divided into magnetically independent segments. The number of segments (N_a) is an additional design parameter, and the author's have investigated designs from 40 to 100 segments.

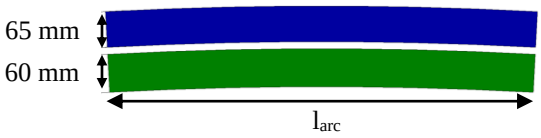

Figure 2: Segment for 6º arc for a 60 segment machine

The large diameter means each single segment closely approximates a linear machine, Figure 2. The segment can be analysed as an individual rotary machine covering 360 mechanical degrees by wrapping the segment to form a rotary model. This is magnetically valid by maintaining the pole pitch to air gap length ratio. The process of approximating a single segment to its linear equivalent and a full 360 degree machine rotary model is shown in Figure 3.

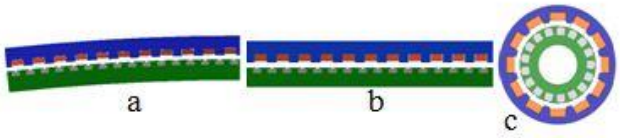

Figure 3: (a) segment of full size machine (b) linear equivalent (c) rotary model of the individual segment, preserving the airgap.

The end effects of the linear segment are considered to be negligible due to the symmetry of adjacent segments forming a rotary machine. In this manner, it is possible to design each machine segment using normal rotary machine design theory applied to the individual segments. Only winding configurations that are usable with linear induction machines are considered for the rotary models.

In this design study, the SCIG design is made to fit within the same volume as the PMSG to avoid modification to the outer frame of the turbine. With the rotor concentric to the stator frame l_g = 12 mm, the effect of rotor eccentricity is outside the scope of this paper. Large values of l_g mean a large stator leakage inductance, which in turn causes poor power factor resulting in higher running costs or a more expensive convertor. The stator thickness is restricted so the slots have to be designed in consideration of the core back depth. The rotor thickness is also restricted so the depth of the bars in the rotor also requires consideration.

The PMSG was used to provide the initial parameters for the design. For example the stator and rotor maximum height ($H_{max\text{-}s,r}$). This consists of the core back depth and tooth length, Figure 2 shows $H_{max\text{-}s}$ = 65mm and $H_{max\text{-}r}$ = 60mm. To determine the stator inner diameter (D_{is}) of the small rotary model, the length of the arc (l_{arc}) was equated with the circumference of the small rotary model.

In equation (1) D_{is} is calculated from the stator inner diameter of the large machine (D'_{is}) and the arc angle of the segment (α).With l_g set as constant the new rotor outer diameter (D_{or}) was calculated.

$$D_{is} = \frac{\alpha}{360} . D'_{is} \qquad (1)$$

3. Design Process

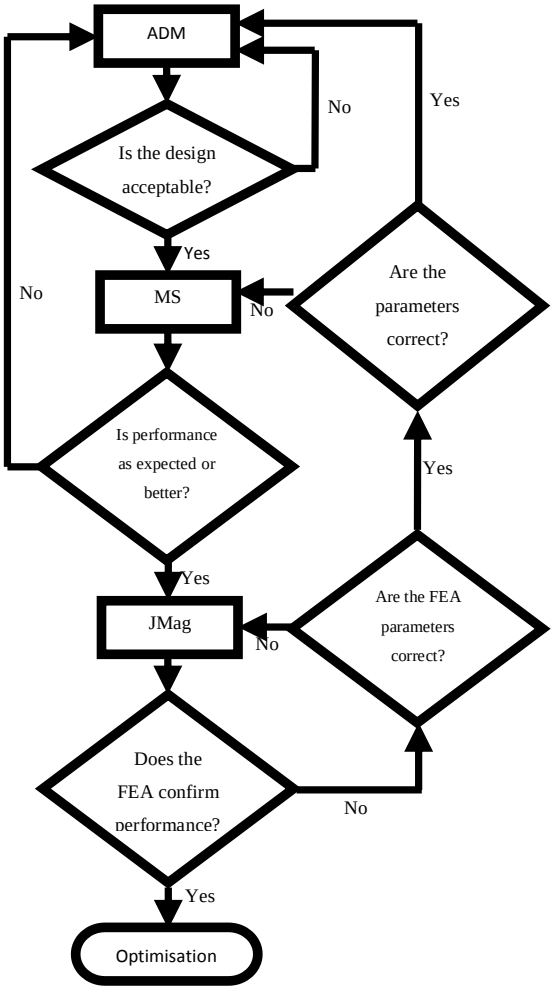

Figure 4: Flow diagram of the design process

The relatively large airgap means normal 'rules of thumb' cannot be followed and it would be unwise to use standard design techniques without validation. Figure 4 shows the design process adopted. An analytical design method (ADM) has been developed based on the output coefficient method [2-4], the performance is predicted from the equivalent

circuit. This allows rapid evaluation of designs for individual induction machine segments. The ADM designs a motor rather than a generator.

To validate the ADM prediction, sample results have been compared to predictions from MotorSolve (MS) software. MotorSolve is a design tool created by Infolytica and uses analytical equations similar to the analytical method in [2] to calculate the performance of the design. The software requires geometrical data and information such as the RMS line voltage (V_{line}) and the number of poles.

Promising designs have then been imported for finite element analysis in Jmag. The paper covers results from 2D transient models, with a view to future commitment to a time intensive 3D transient study.

4. Analytical Design Method

4.1 Main Parameters

Before starting the design process several parameters must be declared. These are: V_{line}, η, PF, f_1, the number of pole pairs (P_1), the mechanical power (P_{mech}) and the number of phases (m).

The axial length (L_a) was calculated using equation (2). The two undefined terms are the EMF coefficient (K_e) and the volume utilisation factor (C_0). The value of C_0 is determined by the calculated apparent air gap power (S_{gap}) and P_1, an approximate value can be found from the graph in [2]. K_e can be calculated using the empirical formula found in [2]. The number of stator slots (N_s) is calculated from equation (3).

$$L_a = \frac{P_1 . K_e . P_{mech}}{\eta . PF . D_{is}^2 . f_1 . C_0} \quad (2)$$

$$N_s = 2 . P_1 . q . m \quad (3)$$

4.2 Magnetic Circuit

With the key physical parameters set, the focus can be shifted to the magnetic characteristics of the design. Equation (4) calculates the flux per pole (φ) based on the pole pitch (τ), the airgap flux density (B_g) and the flux density shape factor (α_i). The result of equation (4) is required to determine the number of turns per phase (N), equation (5). The winding factor (K_{w1}) can be varied to reduce machine harmonics. Both the form factor (K_f) and α_i are determined by the tooth saturation factor (K_{st}). K_{st} is a numerical representation of the effect of the teeth saturation on the airgap magnetic field. With a large value of l_g the effect is negligible therefore K_{st} can be relaxed.

$$\varphi = \tau . L_a . B_g . \alpha_i \quad (4)$$

$$N = \frac{K_e . V_{ph}}{4 . \varphi . K_f . f_1 . k_{w1}} \quad (5)$$

The coils of the designs are star connected to mitigate the triplen harmonics. The line current (I_{line}) is calculated using equation (6). The value of I_{line} with the chosen current density (J_{cu}) sets the cross sectional area of the wire (A_{cu}). Standard round, rectangular and square profile wires with cross sectional areas similar to A_{cu} are selected. A design guideline from [2] states that the slot width (W_{ss}) should be three times greater than l_g. Following this guideline semi closed slots resemble an open slot for the same number of conductors per slot (N_{cs}). Using open slots W_{ss} is a function of the conductor width/diameter (W_c) and the number of conductors orthogonal to the tooth side. The slot height (H_s) is set by the conductor height/diameter and the number of conductors parallel to the tooth. The selected wires arranged in stacks of multiples of N_{cs} eg N_{cs} = 28, W_{ss} = 7*W_c and H_s = 4*H_c. The chosen combination has to follow the guide line, provide a practical tooth width and a suitable value of stator tooth flux density (B_{ts}).

$$I_{line} = \frac{P_{mech}}{\eta . PF . \sqrt{3} . V_{line}} \quad (6)$$

The carter coefficient (K_c) was calculated with the rotor coefficient set as 1.1. The airgap MMF (F_{mg}) was then calculated using equation (7).

$$F_{mg} = \frac{K_c . l_g . B_g}{\mu_0} \quad (7)$$

The stator tooth MMF (F_{mts}) was calculated from the tooth magnetic field strength (H_{ts}) and the length of the tooth (l_t). The rotor tooth MMF (F_{mtr}), equation (8), should have a value close to the value of K_{mts}. This acted as a checkpoint to determine if the stator design was acceptable.

$$F_{mtr} = K_{st} . F_{mg} - F_{mts} \quad (8)$$

4.3 Rotor

The rotor design starts with choosing the number of rotor bars (N_r), various papers have been published concerning the combinations of the N_s and N_r [5-7]. A table of recommended combinations for different number of poles is included in [2].

The SCIG is to be inverter driven, two design guidelines are found in [8] for an appropriate bar shape. The ratio of the upper bar width (W_{rb1}) and the lower bar width (W_{rb2}) should be greater than 0.9, and the ratio of W_{rb2} and the bar height (H_b) should be less than 1.5. Using rectangular bars ensures that the first guideline is always observed.

4.4 Design of a 40 segment machine

The P_{mech} of the large machine is set to the same as the rating of the OpenHydro device, namely, P_{mech} = 2.2 MW. This is divided amongst the 40 segments, per segment and therefore the small rotary machine P_{mech} = 55 kW. To be competitive the efficiency should be greater than 90% however a target efficiency of 80% is more practical. PF was set as 0.5 to account for the large value of l_g. For the initial design N_a is set a value of 40, as this provides an arc angle of 9° comparable to the PMSG arc angle of 5°. Table 1 contains the initial

design parameters and the same parameters for the first valid design, the values for the full machine are included for comparison. Figure 5 shows the initial stator dimensions.

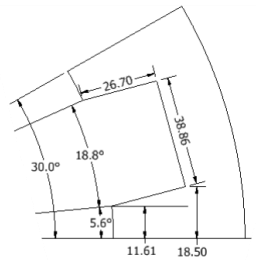

Figure 5: Initial stator slot and tooth dimensions

Table 1: ADM input parameters of the Original 40 (FO) segment machine

Parameters	Units	Initial values	Single segment	Full machine
V_{line}	V_{rms}	415	415	415
P_{mech}	kW	55	55	2200
Ƞ	%	80	80	80
PF	-	0.5	0.6	0.5
F	Hz	33.3	33.3	33.3
N_a	-	40	40	-
P_P	-	1	2	80
n_s	rpm	999	999	25
D_{is}	m	0.356	0.356	14.3
D_{or}	m	0.332	0.332	14.2
L_a	m	0.28	0.28	0.28

4.5 ADM Validation

Results from the ADM have been compared to predicted behaviour from MotorSolve (MS) in Table 2. The efficiency was calculated using equation (9), and the power factor was calculated using equation (10). The difference between the predictions was acceptable – although MS gave a higher efficiency. Higher segment machines were found to have poorer agreement between the predictions and work to investigate and offset this affect is continuing.

$$\eta = \frac{P_{mech}}{P_{mech} + losses} \qquad (9)$$

$$PF = \frac{P_{mech}}{\sqrt{3}.V_{line}.I_{line}.\eta} \qquad (10)$$

Table 2: Predicted performance of the 40 segment designs

		ADM	MS
Ƞ	%	81	86
P_{mech}*N_a	MW	1.96	2
Rated slip	-	0.05	0.05
PF	-	0.6	0.59
I_{line}	A_{rms}	140	137

5. Segment study

Additional designs with differing values of N_a have been created and investigate in MotorSolve. A smaller value of N_a provides more freedom with design parameters such as the choice of P_p, q and N_s, but the segment size and weight is large. A large value of N_a results in smaller and lighter segments however the choice of the design parameters is restricted. Three values have been used to create alternate designs: 40, 60 and 100 segment. These are referred to as FO, SO and HO respectively and are shown in Figure 6. The 40 segment design has 4 poles and both the 60 and 100 segment designs are 2 pole machines. These designs hence represent 60, 80 and 100 pole pair machines.

Table 3: Predicted performance of the designs

Pole pairs		80	60	100
N_a	-	40	60	100
Ƞ	%	86	91.3	86.3
P_{mech}*N_a	MW	2	1.99	2
Rated slip	-	0.05	0.03	0.07
PF	-	0.59	0.56	0.49
I_{line}	A_{rms}	137	89.6	66
P_p	-	2	1	1

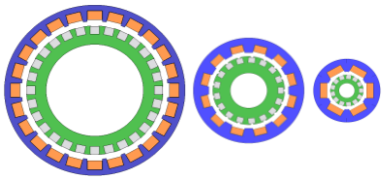

Figure 6: Rotary model of single segment for the Original design for 40(FO), 60(SO) and 100 (HO) segment machines.

The equivalent rotary model of single segments in the 40, 60 and 100 segment machines are shown in Figure 6. The 40 segment machine covers and arc of 9 mechanical degrees in the full machine and is hence larger than the 100 segment machine which covers just 3.6 degrees. Table 3 shows the predicted performance of the designs from MotorSolve. Of these the 60 segment design has the highest, and hence this was taken forward for detailed design. As this design had lowest number of poles, it also had the largest pole width to air gap ratio, believed to be the cause of the superior performance.

6. FEA study of 60 segment machine

To validate the predictions from MotorSolve the FEA software JMag was used to build a 2D rotary model of individual segments. **Error! Not a valid bookmark self-reference.** shows results for the Original Sixty segment design, SO. In comparison to Table 3, the predicted efficiency from the FEA is 4.3% lower than the MotorSolve model and the power factor is 10% lower. The SO design is, however, shown capable of generating the desired P_{mech} and exceeds the target efficiency.

Table 4: Design performance from FEA

		SO
Ƞ	%	87
$P_{mech}*N_a$	MW	1.99
Rated slip	-	0.03
PF	-	0.46
I_{line}	A_{rms}	116

6. Detailed Design Study of 60 segment design in FEA

The design of To validate the predictions from MotorSolve the FEA software JMag was used to build a 2D rotary model of individual segments. **Error! Not a valid bookmark self-reference.** shows results for the Original Sixty segment design, SO. In comparison to Table 3, the predicted efficiency from the FEA is 4.3% lower than the MotorSolve model and the power factor is 10% lower. The SO design is, however, shown capable of generating the desired P_{mech} and exceeds the target efficiency.

Table 4 has been demonstrated as a workable machine with efficiency approaching 90%. Detailed investigation to improve performance by investigating design parameters was taken forward using 2D FEA. Turn number, voltage, current, rotor bar number and slots per pole were all varied according to the work flow shown in Figure 7. The Sixty segment Re-designs are arranged numerically with the prefix of SR, shown in Table 5 and Figure 8.

Table 5: Detailed designs for the 60 segment

design	investigation	Design aim	V_{line} V_{rms}	I_{line} A_{rms}	Rotor bars	Slots per phase
SR-1	Increased turns per phase	reduce magnetisation current	415	105	17	2
SR-2	Increased the line voltage.	to reduce the rated current	690	65	17	2
SR-3	Increased number of rotor bars	reduce vibration and noise	690	107	18	2
SR-4	Increased	improve	690	53	16	3
	slots per pole per phase	the airgap MMF waveform.				

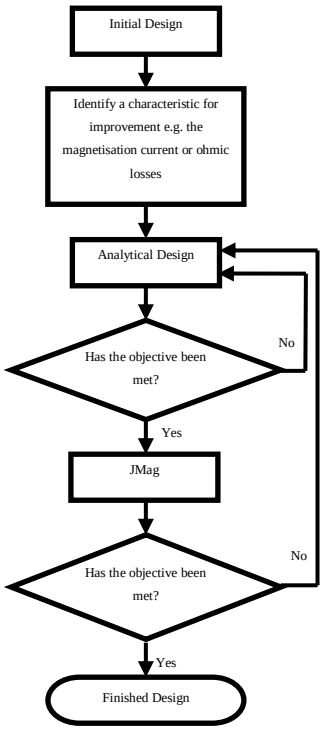

Figure 7: Optimisation process

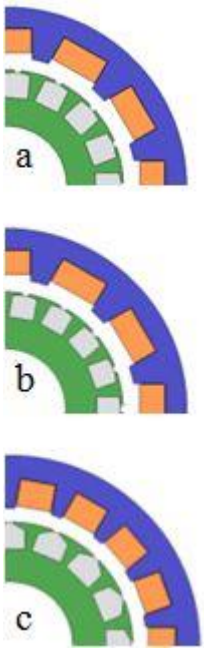

Figure 8: (a) SO (b) SR-3 (c) SR-4

Table 6: Optimised designs

		SO	SR-1	SR-2	SR-3	SR-4
η	%	87	89	87	88	87
P_{mech}	kW	33.2	37.31	37.65	36.11	36.09
Rated slip	-	0.03	0.03	0.03	0.03	0.05
PF	-	0.46	0.56	0.56	0.32	0.61
I_{line}	A_{rms}	116	105	65	107	53
V_{line}	V_{rms}	415	415	690	690	690
Stability	-	0.54	0.6	0.72	0.51	0.91

Results of the four redesigns are shown in Table 6. SR-3 is discarded due to the low operating power factor. Stability is defined as the ratio of rated to peak torque. A lower stability ratio indicates the machine is less likely to fall into the unstable operation region of the torque-slip graph. SR-4, with the highest stability ratio, is operating close to the peak torque and is discarded. SR-1 has the highest efficiency of the remiaing machines and will be taken forward for construction, the slot dimensions are shown in Figure 9.

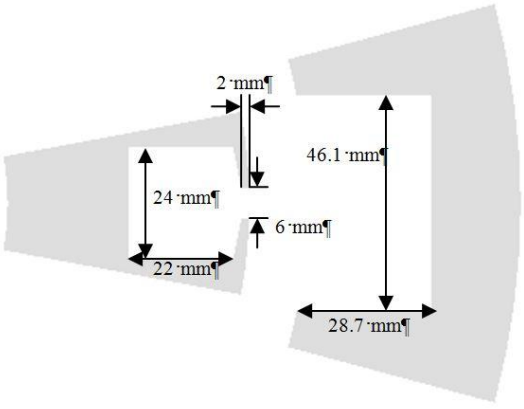

Figure 9: SR-1 stator and rotor slot dimensions

7. Conclusion

The design of an induction generator for use in a tidal turbine has been investigated. An analytical model has been developed and validated at low pole numbers against Motorsolve software. At higher pole numbers, conventional machine design theory diverges from software results, and Motorsolve was hence used to investigate higher pole number machines. The Lowest pole machine, consisting of sixty segments, 60 pole pairs, was taken forward in 2D FEA. Four alternative sixty segment designs were presented, of which one gave the best performance in terms of stability, power factor and efficiency.

Compared to the benchmark permanent magnet synchronous generator, the power factor of the induction machine is worse due to the large air gap length forced by mechanical constraints of the application. The advantages of simple robust construction in the absence of permanent magnets must be considered against the drop in efficiency and power factor associated with the induction machine. With the cost of convertors reducing this in time may become a non-issue.

References

[1] N. J. Baker, S. Cawthorne, E. Hodge, and E. Spooner, "3D modelling of the generator for OpenHydro's tidal energy system," in *Power Electronics, Machines and Drives (PEMD 2014), 7th IET International Conference on*, 2014, pp. 1-6.

[2] I. Boldea and S. A. Nasar, *The induction machines design handbook*, 2nd ed. Boca Raton, FL: CRC Press/Taylor & Francis, 2010.

[3] M. G. Say, *The performance and design of alternating current machines; transformers, three-phase induction motors and synchronous machines*, 3rd ed. London,: Pitman paperbacks, 1968.

[4] L. Lagron, R. C. Simpson, and M. G. Say, *Polyphase induction motors, their theory, calculation, and application*. London, Glasgow,: Blackie & son limited, 1931.

[5] I. K. Pallis, K. N. Gyftakis, and J. C. Kappatou, "FEM study of the bar number impact on the stator core losses of the cage induction motor," in *Industrial Electronics Society, IECON 2013 - 39th Annual Conference of the IEEE*, 2013, pp. 2863-2868.

[6] G. Kron, "Induction Motor Slot Combinations Rules to Predetermine Crawling, Vibration, Noise and Hooks in the Speed-Torque Curve," *American Institute of Electrical Engineers, Transactions of the*, vol. 50, pp. 757-767, 1931.

[7] J. Le Besnerais, V. Lanfranchi, M. Hecquet, and P. Brochet, "Optimal Slot Numbers for Magnetic Noise Reduction in Variable-Speed Induction Motors," *Magnetics, IEEE Transactions on*, vol. 45, pp. 3131-3136, 2009.

[8] Z. M. Zhao, S. Meng, C. C. Chan, and E. W. C. Lo, "A novel induction machine design suitable for inverter-driven variable speed systems," *Energy Conversion, IEEE Transactions on*, vol. 15, pp. 413-420, 2000.